Spectroscopic characterization of the blue and red complexes in reduced SO_2 solutions in HMPA

Elisabeth Potteau,[a] Eric Levillain*[b] and Jean-Pierre Lelieur*[a]

[a] *Laboratoire de Spectrochimie Infrarouge et Raman (LASIR, CNRS UMR 8516), Hautes Etudes Industrielles (HEI), 13, rue de Toul, 59046 Lille cedex, France. Fax: +33 3 28 38 48 04; E-mail: jean-pierre.lelieur@*hei*.fr.*

[b] *Ingénierie Moléculaire et Matériaux Organiques (IMMO, CNRS UMR 6501), Université d'Angers, 2, boulevard Lavoisier, 49045 Angers cedex, France. E-mail: eric.levillain@univ-angers.fr.*

Received (in Montpellier, France) 3rd May 1999, Accepted 30th August 1999

Polythionite solutions $Li(SO_2)_n$–HMPA, where SO_2 is reduced chemically by lithium, have been investigated using ESR and spectrophotometry. The variation of the Li/SO_2 ratio allows us to modify the distribution of the reduced species, which has led to the identification and characterization of these species. It is shown that the 595 nm absorption band must be assigned to a new species: $S_4O_8^{2-}$, the dimer of $S_2O_4^{-\cdot}$. In previous works, this absorption band was assigned to $S_2O_4^{-\cdot}$, named the blue complex for this reason. We show that the blue complex is not $S_2O_4^{-\cdot}$, but its dimer. The equilibrium constants for the reactions between the reduced species: the dimerization of $SO_2^{-\cdot}$, that of $S_2O_4^{-\cdot}$, and the formation of $S_2O_4^{-\cdot}$ by reaction between SO_2 and $SO_2^{-\cdot}$, were determined, thus allowing the concentrations of all the species in a given solution to be calculated. In the presence of a supporting electrolyte, the red complex $S_3O_6^{2-}$ is observed and it is shown, from spectroelectrochemical experiments, that this species is formed by reaction between $SO_2^{-\cdot}$ and $S_2O_4^{-\cdot}$.

Sulfur dioxide is involved in several types of batteries, in addition to Li/SO_2 batteries:[1] for example, Li ion batteries now often contain SO_2 as an additive.[2] In addition, the sulfur dioxide radical anion, $SO_2^{-\cdot}$, is widely used as a reagent in organic electrosynthesis.[3,4] To improve the conception of these batteries, or to increase the reaction yields, a good understanding of the reduction of SO_2 in non-aqueous solvents is required.

This reduction has been studied for a long time,[5,6] but there is no general agreement about its mechanism. Two main approaches have been used. Some authors have studied SO_2 solutions by electrochemical techniques,[7–15] such as cyclic voltammetry or chronopotentiometry. Others have studied electrolyzed solutions, using various spectroscopic techniques: ESR,[5,12,16–18] spectrophotometry,[7,9,12,15] Raman spectroscopy.[19]

These studies have shown that the first step of the reduction of SO_2 is a one-electron transfer according to the reaction:

$$SO_2 + e^- \rightleftharpoons SO_2^{-\cdot} \quad (1)$$

The $SO_2^{-\cdot}$ radical anion produced undergoes a number of follow-up reactions, and several reaction paths appear to be in competition. It is generally agreed that $SO_2^{-\cdot}$ is in equilibrium with its dimer, the dithionite ion $S_2O_4^{2-}$:

$$2SO_2^{-\cdot} \rightleftharpoons S_2O_4^{2-} \quad (2)$$

In addition to $SO_2^{-\cdot}$, a second stable radical species has been observed since the first studies[5,16] and was identified as $(SO_2)_xSO_2^{-\cdot}$, but the value of x has long been uncertain. However, since the work of Gardner *et al.*,[13] it is accepted that $x = 1$, giving the formula $S_2O_4^{-\cdot}$. This species is formed through the following reaction:

$$SO_2 + SO_2^{-\cdot} \rightleftharpoons S_2O_4^{-\cdot} \quad (3)$$

The early studies evidenced the presence of colored species:[6] a blue complex and a red one. The blue complex, absorbing around 580 nm, was identified as the $(SO_2)_xSO_2^{-\cdot}$ radical, formed by reaction (3). The existence of this species is accepted by nearly all authors, except by Bonnaterre and Cauquis,[7] and Harrison *et al.*[20] However, the electrochemical behavior of the blue complex is not well understood.

The existence of a red complex is also mentioned in a few studies, and does not seem to depend on the solvent: it is observed in DMF,[8,12,18] DMSO,[10,15] *N*-methylpyrrolidinone (NMP)[18] and acetonitrile.[18] The red complex absorbs at 490 nm and does not display any ESR signal. Nearly all authors who identify it agree on the formula $S_3O_6^{2-}$, except Anantaraman *et al.*,[18] who suggest the formula $S_4O_8^{2-}$ in acetonitrile, and $S_3O_6^{2-}$ in DMF and NMP. This species is characterized by spectrophotometry,[8,12,15] but its electrochemical behavior is unknown. It can be formed by two reactions:[12]

$$S_2O_4^{-\cdot} + SO_2^{-\cdot} \rightleftharpoons S_3O_6^{2-} \quad (4)$$

$$SO_2 + S_2O_4^{2-} \rightleftharpoons S_3O_6^{2-} \quad (5)$$

but Martin and Sawyer[8] concluded that reaction (5) is predominant.

However, the mechanism composed of reactions (1)–(5) explains only partly the experimental results, and seems to be incomplete. In addition to the species mentioned above, several other reactions have been proposed, but they are rather controversial. For instance, a few authors have considered the disproportionation of $SO_2^{-\cdot}$ into SO and SO_3^{2-},[10,12–15] but little experimental proof was given.

The experimental approaches followed in the previous studies do not seem to allow a satisfactory understanding of the reduction mechanism of sulfur dioxide, and give evidence for its complexity. The present study uses an original approach to stabilize the reduced species of sulfur dioxide. We have recently shown[21] that these species, resulting from the chemical reduction of sulfur dioxide by lithium, can be stabilized in hexamethylphosphoramide (HMPA). The polythionite

solutions $Li(SO_2)_n$–HMPA obtained by this method can be investigated by various spectroscopic techniques. The adjustment of the SO_2/Li ratio, that is of n, allows the relative concentrations of the reduced species in these solutions at equilibrium to be modified.

In this paper, we present the spectroscopic study of the polythionite solutions. The reduced species have been identified and characterized using spectrophotometry and ESR spectroscopy. The quantitative study allowed us to determine the equilibrium constants of the reactions between these species.

The polythionite solutions are prepared without a supporting electrolyte. However, for electrochemical studies the solutions must contain a supporting electrolyte. The polythionite solutions have first been studied in the absence of a supporting electrolyte, because this allows one to reach higher concentrations. Then, the influence of the addition of a supporting electrolyte has been examined.

Experimental

Materials

The choice of hexamethylphosphoramide (HMPA) as a solvent, and of lithium to reduce SO_2, has been discussed elsewhere.[21] HMPA (Aldrich, 99%) is dried on NaH for at least 24 h, then distilled twice at 100 °C.[22] SO_2 (Air Liquide, >99.7%) is purified on H_2SO_4, then on P_2O_5.[23] Lithium (Fluka, 99%) is used as received. Tetraethylammonium perchlorate (TEAP, Fluka, >99%) is dried under vacuum at 150 °C for at least 24 h.

Preparation of polythionite solutions

All solutions are prepared and stored in a glove box with a dry oxygen-free argon atmosphere. A concentrated SO_2–HMPA solution is first prepared by condensing SO_2 on HMPA at 77 K. The amount of condensed SO_2 is determined by volumetry of SO_2 in the gas phase. A weighed mass of lithium is then added to this solution. It can reasonably be considered that lithium first dissolves in HMPA to give solvated electrons, which then reduce SO_2. The overall reaction for the preparation of polythionite solutions is the following:[9]

$$Li + nSO_2 \rightarrow Li^+ + SO_2^{-\cdot} + (n-1)SO_2 \quad \text{with } n \geqslant 1 \quad (6)$$

The adjustment of the SO_2/Li ratio allows us to modify the distribution of reduced species in solution, and therefore, to study them selectively at equilibrium. It is important to note that the stoichiometry n is always larger than (or equal to) one. Under these conditions, no excess of lithium remains in solution under the form of solvated electrons. This avoids problems due to the rather weak stability of solvated electrons in HMPA at room temperature.[24] In order to minimize losses of SO_2, the volume of the gas phase relative to the volume of the liquid phase was kept as small as possible. The value of n for each solution investigated has been calculated by taking into account the SO_2 content in the gas phase.

The polythionite $Li(SO_2)_n$–HMPA solutions obtained by this method are blue, or colorless or slightly yellow when n is close to one. As previously shown,[21] these solutions are stable.

Apparatus

ESR spectra were recorded with an ESP 300 spectrometer (Bruker) in the X-band frequency range, equipped with a TE_{102} cavity. The Suprasil® quartz cells are cylindrical and their inner diameters, close to 1 mm, were calibrated with mercury in order to perform a quantitative study of the experimental signals. All experiments were run with a 100 kHz modulation frequency, a 96 mG modulation amplitude and 8 mW of microwave power, which was verified to be lower than saturation conditions. The spectra were recorded at 295 ± 0.1 K with a standard variable-temperature cryostat using cold nitrogen gas. A standard DPPH sample was used for the field calibration of the spectrometer.

UV/visible absorption spectra were recorded using a Perkin-Elmer Lambda 19 UV/visible NIR spectrophotometer. The spectra were recorded at room temperature between 230 (solvent cut-off) and 2000 nm. The large concentration range investigated implied the use of optical cells with different pathlengths, between 0.1 and 5 mm. In order to simplify the presentation of the data, the absorbance values are divided by the optical pathlength expressed in cm. The decomposition of the spectra has been described previously.[25] The spectra are displayed on the wavelength scale, but the decomposition calculations were performed on the energy scale.

The experimental setup for the spectroelectrochemistry experiments has been previously described.[26] From the electrochemical viewpoint, the cell is a classical three-electrode cell. The working electrode is a 5 mm diameter platinum disk, polished to a mirror finish. The ferrocenium/ferrocene (Fc^+/Fc) couple is used as an internal potential reference, according to the procedure recommended by IUPAC.[27]

Results and discussion

The polythionite solutions $Li(SO_2)_n$–HMPA have been studied *vs.* n for $[Li^+] = 0.05$ mol dm^{-3}, and *vs.* $[Li^+]$ for $n = 1.5$. Two spectroscopic techniques have been used: ESR and spectrophotometry. Raman spectroscopy did not give any exploitable spectra because we observed some fluorescence, which has already been mentioned by Adams *et al.*,[19] and because the solutions are too dilute.

The aims of this study were to identify the reduced species, and to determine the equilibrium constants of the reactions between these species. By using spectrophotometry, the absorption bands of each species have been identified, as well as their molar absorption coefficients. This provides a better characterization of the reduced species, which is an important point in the study of the reduction mechanism of sulfur dioxide.

ESR study of polythionite solutions

The ESR spectrum of a polythionite solution is composed of a single line, or the sum of two lines, depending on the value of n. The study at low temperatures (down to 100 K) showed the absence of any other broader line species. The analysis of ESR spectra has been described elsewhere.[28] The ESR spectra were fitted to one or two Lorentzian components, by using the non-linear least-squares algorithm of Levenberg–Marquardt.[29] and the area of each component was determined from the fitted parameters. The adjustment of the Lorentzian profiles to the experimental spectra is very satisfactory for all the spectra, and the residue is always of the same order of magnitude as the noise. The average values of the parameters of these two ESR signals are given in Table 1.

For $n = 1$, the ESR spectrum displays one single broad Lorentzian line. For n larger than 1 and lower than about 1.25, the ESR spectrum displays two components [Fig. 1(*a*)]. No half-field signal was observed, indicating that there is no interaction between the two radicals. The broad signal at $g = 2.0043$ is the most intense. A signal with a very similar g

Table 1 Parameters of the ESR signals observed in polythionite solutions

	g	ΔH_{pp}/G	Species
"broad signal"	2.0043 ± 0.0002	3.22 ± 0.02	$SO_2^{-\cdot}$
"narrow signal"	2.005 45 ± 0.000 05	0.38 ± 0.02	$S_2O_4^{-\cdot}$

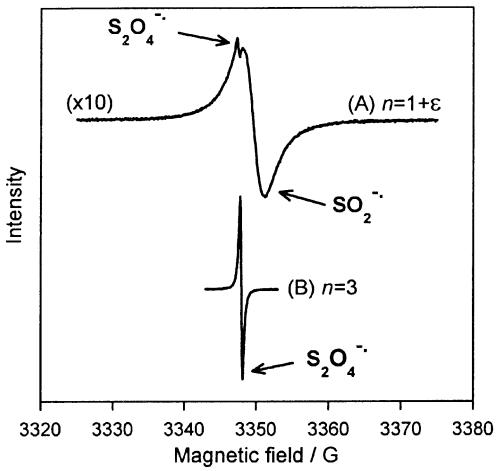

Fig. 1 ESR spectra of $Li(SO_2)_n$–HMPA solutions with $[Li^+] = 0.05$ mol dm^{-3}. (*A*) $n = 1 + \varepsilon$ with $\varepsilon < 0.01$ (intensity × 10): both signals of $SO_2^{-\cdot}$ and $S_2O_4^{-\cdot}$ are observed; (*B*) $n = 3$: only the narrow line of $S_2O_4^{-\cdot}$ is observed.

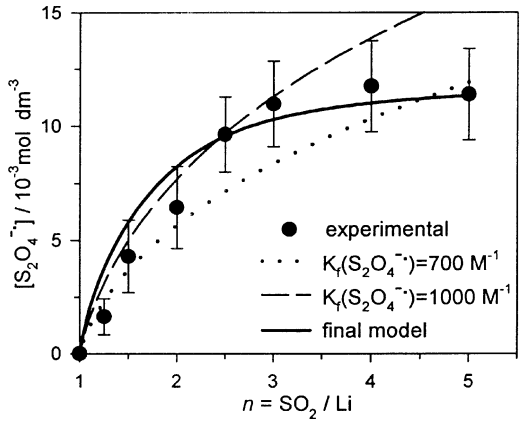

Fig. 2 Concentration of $S_2O_4^{-\cdot}$ *vs.* n in $Li(SO_2)_n$–HMPA solutions with $[Li^+] = 0.05$ mol dm^{-3}. For each value of n, at least five solutions were investigated, but only the mean value is plotted. The error bars take into account both the standard deviation of these measurements and the error of the decomposition calculation. (···) and (– – –): Calculated from the model involving reactions (2), (3), and (8) (without $S_4O_8^{2-}$), for two values of $K_f(S_2O_4^{-\cdot})$. The line does not fit well the experimental points. (——): Calculated from the model involving reactions (2), (3), (8) and (9) ($S_4O_8^{2-}$ taken into account). The adjustment is then satisfactory.

value and linewidth was observed for a $Na_2S_2O_4$–HMPA solution. This broad signal is assigned to the $SO_2^{-\cdot}$ radical.[5,12,17,21] The values obtained for the g factor and the linewidth are similar to those measured in other solvents.[5,12,17,30] The area of this ESR signal decreases when n is increased, and this signal disappears for $n > 1.25$. This is not surprising because when n increases, SO_2 is added to the solution, and $SO_2^{-\cdot}$ is then consumed through reaction (3).

In order to determine the absolute concentration of the radical species in the solutions, the ratio between the ESR signal area and the radical concentration was determined by following the previously described procedure,[31] using Li_2S_6–DMF solutions. From the area of its ESR signal, the concentration of $SO_2^{-\cdot}$ in a polythionite solution with $n = 1$ was found to be $(6.1 \pm 0.6) \times 10^{-4}$ mol dm^{-3}. This low value (compared to $[Li^+] = 5 \times 10^{-2}$ mol dm^{-3}) confirms the existence of the dimer species $S_2O_4^{2-}$. The charge balance can be written:

$$[Li^+] = [SO_2^{-\cdot}] + 2[S_2O_4^{2-}] \quad (7)$$

It gives $[S_2O_4^{2-}] = 24.7 \times 10^{-3}$ mol dm^{-3}. This allows the equilibrium constant for the dimerization of $SO_2^{-\cdot}$ [reaction (2)] to be calculated: we obtain $K_{dim.}(SO_2^{-\cdot}) = (6.6 \pm 2.0) \times 10^4$ mol^{-1} dm^3. This confirms that this equilibrium strongly favors $S_2O_4^{2-}$. This value has never been reported in the literature for HMPA, but is of the same order of magnitude as the values obtained in other non-aqueous solvents, such as DMF or DMSO.[7,14]

In polythionite solutions, the solubility of $S_2O_4^{2-}$ is slightly higher than 25×10^{-3} mol dm^{-3}, while $Na_2S_2O_4$ is almost insoluble in HMPA.[30] This seems to be rather strange, since these two solutes are very similar: the only difference is the nature of the cation (Li^+ or Na^+), but both cations are small. It has been observed that dithionite salts with small cations are much less soluble in non-aqueous solvents than those with large cations.[30] The high solubility of $S_2O_4^{2-}$ in the case of $Li(SO_2)_n$ solutions is rather surprising and is not presently explained. It could be due either to different conformations of the dithionite anion depending on its environment, as observed by Hödgeman *et al.*,[32] or to an influence of the solvation of the cation on its effective size.

The narrow signal at $g = 2.00545$ increases when n increases, and it is the only signal observed for $n > 1.25$ [Fig. 1(*b*)]. This signal is assigned to $S_2O_4^{-\cdot}$.[5,12,16,17] Again, its characteristics are quite similar to those obtained previously.[5,12,16,17,21] Its area increases with n up to $n \approx 2$, and then reaches a constant value (Fig. 2). At $n = 2$ there is a one-fold excess of SO_2, which confirms the global stoichiometry $SO_2 \cdot SO_2^{-\cdot} = S_2O_4^{-\cdot}$. The signal does not decrease for $n > 2$, indicating the absence of less reduced species at equilibrium ($S_xO_{2x}^{-\cdot}$ with $x > 2$ does not exist, nor does its dimer).

In order to explain the variation of the concentration of $S_2O_4^{-\cdot}$ *vs.* n, it is necessary to build a model taking into account at least three reactions. The dimerization of $SO_2^{-\cdot}$ [reaction (2)] and the formation of $S_2O_4^{-\cdot}$ from $SO_2^{-\cdot}$ and SO_2 [reaction (3)] have already been discussed. The third reaction is the dimerization of SO_2: the spectrophotometric study of SO_2–HMPA solutions[25] demonstrated the existence of a dimer species, S_2O_4:

$$2SO_2 \rightleftharpoons S_2O_4 \quad (8)$$

with $K_{dim.}(SO_2) = 77 \pm 25$ mol^{-1} dm^3. This equation must be taken into account because it decreases the amount of free SO_2 in the solution.

The only unknown parameter in the model composed of reactions (2), (3) and (8) is the equilibrium constant for the formation of $S_2O_4^{-\cdot}$, $K_f(S_2O_4^{-\cdot})$. Using this model, $[S_2O_4^{-\cdot}]$ can be calculated for any value of n and $[Li^+]$, provided that a value is assigned to $K_f(S_2O_4^{-\cdot})$. However, for all values of $K_f(S_2O_4^{-\cdot})$, the calculated curve of $[S_2O_4^{-\cdot}]$ *vs.* n does not reproduce the experimental behavior (Fig. 2): $[S_2O_4^{-\cdot}]$ never reaches a constant value when n increases, but continues to increase. It is then necessary to take into account one more reaction in the model, which will result in a lowering of $[S_2O_4^{-\cdot}]$ for high values of n.

This new reaction could be the formation of $S_3O_6^{2-}$, the red complex, through reaction (4), but it will be shown below that this species has an absorption band at 500 nm, which is not observed here. Consequently, the necessary decrease of $[S_2O_4^{-\cdot}]$ for high values of n can occur through a disproportionation and/or a dimerization of this species. The only realistic disproportionation mechanism of $S_2O_4^{-\cdot}$ is:

$$2S_2O_4^{-\cdot} \rightleftharpoons S_2O_4^{2-} + S_2O_4 \quad (9)$$

Obviously, this reaction is thermodynamically superfluous: it is a combination of reactions (2), (3) and (8). Consequently, the introduction of this reaction cannot modify the variations of $[S_2O_4^{-\cdot}]$ *vs.* n. It must also be noted that reaction (9), which can be considered as an electron transfer reaction, can be discarded on the basis of structural considerations. The $S_2O_4^{2-}$

molecule is composed of two $SO_2^{-\cdot}$ units linked by a S–S bond.[32,33] The structure of $S_2O_4^{-\cdot}$ is more controversial but *ab initio* calculations[34–36] indicate that SO_2 and $SO_2^{-\cdot}$ are linked by a S–O or O–O bond. These structural differences imply that the disproportionation mechanism of eqn. (9) is unlikely. Even if this reaction can be written, the structural constraints imply that it must involve several intermediate stages [*i.e.*, eqns. (2), (3) and (8)].

Consequently, the decrease of $[S_2O_4^{-\cdot}]$ can only occur through the dimerization of $S_2O_4^{-\cdot}$:

$$2S_2O_4^{-\cdot} \rightleftharpoons S_4O_8^{2-} \quad (10)$$

The existence of this species has never been considered before, but radicals in solution often dimerize; moreover, both SO_2 and $SO_2^{-\cdot}$ do.

The model then involves four reactions [reactions (2), (3), (8) and (10)], and two unknown equilibrium constants, $K_f(S_2O_4^{-\cdot})$ and $K_{dim.}(S_2O_4^{-\cdot})$. The concentration of $S_2O_4^{-\cdot}$ calculated with this model has been fitted (Fig. 2) to the experimental data of $[S_2O_4^{-\cdot}]$ *vs.* *n*, by using a non-linear least-squares procedure. The numerical adjustment gives $K_f(S_2O_4^{-\cdot}) = 2000 \pm 600$ mol^{-1} dm^3 and $K_{dim.}(S_2O_4^{-\cdot}) = 130 \pm 50$ mol^{-1} dm^3. The quality of the adjustment has been checked by using ANOVA and the *F* test for the lack-of-fit.[37] The absolute experimental uncertainty was determined by making replicate measurements, and the *F* value was calculated as the ratio of the mean sum of squares due to lack-of-fit to that due to experimental uncertainty. This value was then compared to the critical one, given in the *F* distribution table, at the chosen significance level. The *F* test is passed, which shows that the quality of the adjustment is satisfactory, taking into account the experimental uncertainty.

The values obtained for the equilibrium constants cannot be compared with those we had previously given,[21] because we did not take into account the dimerization of SO_2, and we made the approximation that $SO_2^{-\cdot}$ was totally dimerized. The value obtained for $K_f(S_2O_4^{-\cdot})$ is close to those measured previously, in other solvents.[12,14,17,18] The model involves the minimum number of equations to describe the experimental results. Several other reactions can be written by linear combination of the reactions given here, but they will have no influence on the composition of the solutions.

Spectrophotometric study of polythionite solutions

The absorption spectrum of a polythionite solution with *n* close to 1 and $[Li^+] = 0.05$ mol dm^{-3} is displayed in Fig. 3. The NIR part of the spectrum is not shown, because the only absorption bands observed in this region are those of the solvent. Between 230 and 900 nm, this spectrum is decomposed satisfactorily with two absorption bands (Fig. 3), whose parameters are reported in Table 2. We have observed two bands at the same wavelengths for a $Na_2S_2O_4$–HMPA solution, but the absorbance ratio between the two bands is different for the two types of solutions. Consequently, these bands (Fig. 3) cannot be assigned to the same species, and one of the

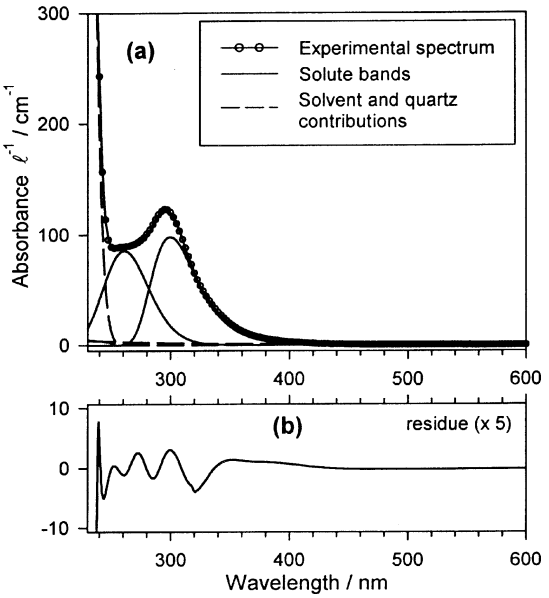

Fig. 3 UV/visible absorption spectrum of a $Li(SO_2)_n$–HMPA solution with $n = 1 + \varepsilon$ ($\varepsilon < 0.01$) and $[Li^+] = 0.05$ mol dm^{-3}. (*a*) Experimental spectrum and decomposition into five Gaussian bands: three for the quartz and solvent contributions, and two for $SO_2^{-\cdot}$ and $S_2O_4^{2-}$, (*b*) Residue of the adjustment. Note that the absorbance has been divided by the optical pathlength.

two bands must then be assigned to $SO_2^{-\cdot}$ and the other one to $S_2O_4^{2-}$: these are the only species present in solution. The previous studies cannot help to assign these bands, because several interpretations have been given. For $SO_2^{-\cdot}$, the only value is that of Kim and Park,[15] at 326 nm. The absorption band of $S_2O_4^{2-}$ has been found at 350 nm,[8] 297 nm,[9] or 355 nm.[15] Another possibility to assign the bands observed at 260 and 300 nm would be to study solutions as a function of concentration, but this method was not conclusive because the concentration range available is too small: if $[Li^+]$ exceeds 0.05 mol dm^{-3}, lithium dithionite precipitates. Thus, we cannot assign each band to a given species, but the study of polythionite solutions with *n* close to 1 shows that $SO_2^{-\cdot}$ and $S_2O_4^{2-}$ have their absorption bands in the UV region.

For $n > 1$ (Fig. 4), several absorption bands are observed, and their absorbance increases with *n*. In the UV region, the two bands observed in polythionite solutions with $n = 1$ are observed for low values of *n*. When *n* increases, an absorption band at about 270 nm is also observed, and for $n > 2$, the absorbance of the solution is too high to be measured. In the NIR region, several absorption bands are observed, but they belong to the solvent. Consequently, the decomposition calculations have only been performed for wavelengths between 370 and 900 nm. In this region, we observe a set of narrow bands around 400 nm, and a broad asymmetrical band at 595 nm. The same model was used for the decomposition of all spectra: the group of bands around 400 nm was decomposed

Table 2 Parameters of the absorption bands deduced from the decomposition of the spectra of polythionite solutions

λ/nm	$\Delta\bar{\nu}$/cm^{-1}	Lineshape	Asymmetry parameter	Assignment	ε/cm^{-1} mol^{-1} dm^3
260 ± 1	6540 ± 40	Gaussian		$SO_2^{-\cdot}$ or $S_2O_4^{2-}$	—
300.0 ± 0.5	4920 ± 10	Log-normal	−0.243 ± 0.005	$SO_2^{-\cdot}$ or $S_2O_4^{2-}$	—
391 ± 1	2300 ± 300	Gaussian		$S_4O_8^{2-}$	8900 ± 3000
398.0 ± 0.4	960 ± 150	Gaussian		$S_4O_8^{2-}$	8100 ± 2800
411.0 ± 0.3	770 ± 40	Gaussian		$S_4O_8^{2-}$	12500 ± 4300
498 ± 3	6000 ± 800	Gaussian		$S_3O_6^{2-}$	—
595.7 ± 0.6	4300 ± 80	Log-normal	−0.20 ± 0.03	$S_4O_8^{2-}$	9500 ± 3300

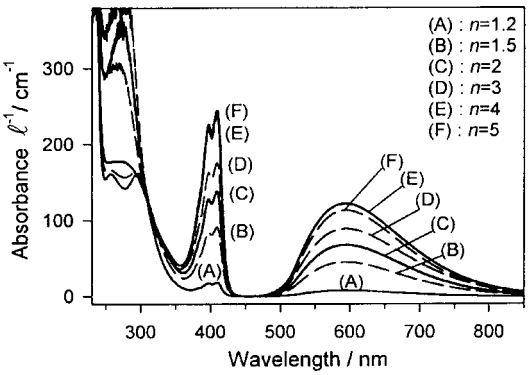

Fig. 4 UV/visible absorption spectra of $Li(SO_2)_n$–HMPA solutions with $[Li^+] = 0.05$ mol dm^{-3} and different values of n. In the visible range, we observe a broad asymmetrical band at 595 nm, and a set of narrow bands around 400 nm. The absorbance of these bands increases with n. Note that the absorbance has been divided by the optical pathlength.

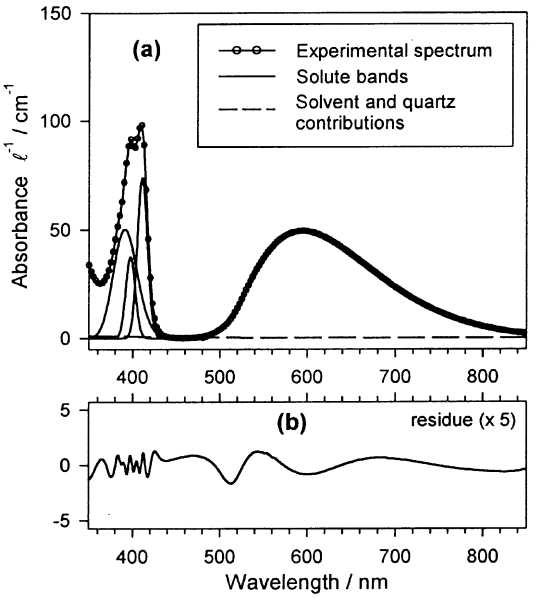

Fig. 5 Decomposition of the absorption spectrum in the visible range of a $Li(SO_2)_n$–HMPA solution with $n = 2$ and $[Li^+] = 0.05$ mol dm^{-3}. The UV part of the spectrum involves too many overlapping bands to allow a satisfactory decomposition. (*a*) Experimental spectrum and decomposition, (*b*) residue of the adjustment. Note that the absorbance has been divided by the optical pathlength.

into three Gaussian bands, and the broad band at 595 nm was described with a log-normal lineshape.[38] The parameters of these bands are reported in Table 2; they do not depend on n or $[Li^+]$, over a wide range of concentration and n values. Fig. 5 shows one of the spectra after decomposition; the good quality of the fit is indicated by the residue.

The absorbance of these four bands follows the same variation with n [Fig. 6(*a*)] or $[Li^+]$ [Fig. 6(*b*)]. These bands must then be assigned to the same species. From the ESR study, the equilibrium constant of each reaction was determined. This allows one to calculate the concentration of each species *vs.* n [Fig. 6(*c*)] or $[Li^+]$ [Fig. 6(*d*)]. The only species whose concentration variations are similar to those of the absorbance is $S_4O_8^{2-}$. Consequently, these bands must be assigned to

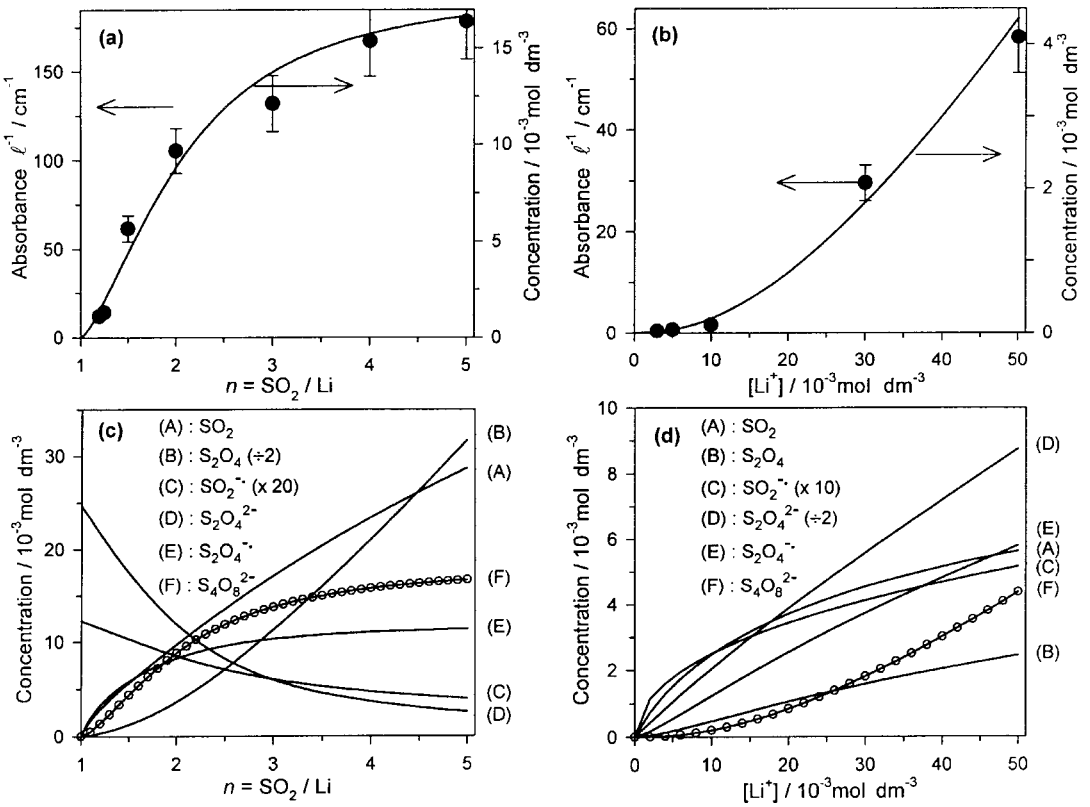

Fig. 6 (*a*, *b*) Absorbance of the 411 nm band (●, left axis scale), obtained by the decomposition of the UV/visible spectra, and concentration of $S_4O_8^{2-}$ (——, right axis scale), calculated using the model composed of reactions (2), (3), (8) and (9), and the equilibrium constants obtained in the ESR study. (*a*) $Li(SO_2)_n$–HMPA solutions with $[Li^+] = 0.05$ mol dm^{-3} *vs.* n, (*b*) $Li(SO_2)_n$–HMPA solutions with $n = 1.5$ *vs.* $[Li^+]$. For each value of n, at least three solutions were investigated, but only the mean value is plotted. The error bars take into account both the standard deviation of these measurements and the error of the decomposition calculation. The two plots are superposed by adjusting the scales of the two axes. By comparing the two ordinate scales, the molar absorption coefficient of the absorption band is deduced. The same procedure is applied for the three other bands. (*c*, *d*) Concentration of each species in $Li(SO_2)_n$–HMPA solutions: (*c*) *vs.* n for $[Li^+] = 0.05$ mol dm^{-3}, and (*d*) *vs.* $[Li^+]$ for $n = 1.5$. These values are calculated using the equilibrium constants obtained in the ESR study. The only species whose concentration follows the same variation as the absorbance of the four bands is $S_4O_8^{2-}$ (–○–○–).

$S_4O_8^{2-}$. In previous works,[8,9,12,15] they were assigned to $S_2O_4^{-\cdot}$, which had been named the blue complex, due to its absorption band at 595 nm. The variation of $[S_2O_4^{-\cdot}]$ with n for $[Li^+] = 0.05$ mol dm^{-3} [Fig. 6(*c*)] is not very different from that of the absorbance [Fig. 6(*a*)], but for $n = 1.5$, the variations of $[S_2O_4^{-\cdot}]$ [Fig. 6(*d*)] and the absorbance [Fig. 6(*b*)] with $[Li^+]$ are completely different. These absorption bands can certainly not be assigned to $S_2O_4^{-\cdot}$. This conclusion is in opposition with those of the previous works, but it is also the first time that the existence of $S_4O_8^{2-}$ has been considered. The observation that the absorbance of each band follows the same variation as $[S_4O_8^{2-}]$ is a very important indication for the validity of our model: this shows that two independent sets of experimental data (ESR and spectrophotometric study) lead to the same conclusion.

The comparison between the absorbance of each band and $[S_4O_8^{2-}]$ [Fig. 6(*a*) and (*b*)] allows the molar extinction coefficient of each band to be estimated (Table 2). No comparison can be made with previous works, because these absorption bands were erroneously assigned to $S_2O_4^{-\cdot}$.

Influence of the addition of a supporting electrolyte

Previous works have shown that the nature of the supporting electrolyte has an influence on the reduction of SO_2.[11,12,14,39] As these authors used only electrochemical methods, they could not study solutions in the absence of a supporting electrolyte. In the present work, the polythionite solutions are prepared chemically, which does not require the use of a supporting electrolyte. The spectroscopic study of these solutions led to the identification and characterization of the reduced species. However, to use this information for the interpretation of the electrochemistry experiments, it is necessary to study polythionite solutions in the presence of a supporting electrolyte.

The supporting electrolyte used in our electrochemistry experiments is TEAP, used in most of the previous studies.[7,8,11–14,17,18] The presence of a supporting electrolyte in the solutions increases the ionic strength, which modifies the distribution of the species by changing the apparent value of the equilibrium constants. When TEAP is added to a polythionite solution, its influence is easily observed: the blue color of the solution immediately turns violet. In the absorption spectra, the only new band is located in the visible region (Fig. 7). The absorbance of this new band increases with [TEAP], that is, with the ionic strength. These conditions favor the complexation of molecules;[40] this band then belongs to a complexed species. Moreover, no new ESR signal is detected, thus indicating that this species is not a radical.

This observation of a new absorption band is not specific to TEAP. The same band is observed with tetrabutylammonium hexafluorophosphate ($TBAPF_6$). This indicates that the corresponding species does not result from a reaction between the reduced species and the salt. However, when the supporting electrolyte is a salt with a small cation, such as LiCl or $LiClO_4$, this band is not observed. Under these conditions, the concentration of the blue complex is also much lower, as are the ESR signals of $SO_2^{-\cdot}$ and $S_2O_4^{-\cdot}$. This means that the major species in the solution are then SO_2, S_2O_4 and $S_2O_4^{2-}$, the non-radical species, which absorb in the UV region. In this case, the dithionite anion is favored relative to other charged species; this was expected from the experiments of Gardner *et al.*[14]

In order to identify the species characterized by this new absorption band, we recorded the absorption spectra of polythionite solutions with $[Li^+] = 0.005$ mol dm^{-3} and [TEAP] = 0.1 mol dm^{-3} *vs.* n. The decomposition of the spectra shows that there is only one new absorption band, characterized by a Gaussian lineshape, with $\lambda_{max} = 498 \pm 3$ nm and $\Delta\bar{\nu} = 6000 \pm 800$ cm^{-1}. Fig. 8 displays the absorbance of this band, obtained by the decomposition of the spectra. In the literature, all experiments were run in the presence of a supporting electrolyte, and several authors have observed the red complex, absorbing at 485–490 nm, in DMF and DMSO.[8,12,15] This species was given the formula $S_3O_6^{2-}$. In HMPA, the absorption band is located at 498 nm, which is slightly different from what was observed in DMF and DMSO, but the maximum absorption wavelength appears to depend on the solvent (485 nm in DMF,[8,12] and 490 nm in DMSO[15]).

This interpretation fits our experimental observations in the case of polythionite solutions in HMPA: $S_3O_6^{2-}$ is not a radical species, which is consistent with the absence of any corresponding ESR signal. Moreover, it is a complexed species, which explains why it is favored when the ionic strength is increased. $S_3O_6^{2-}$ is probably present in polythionite solutions in the absence of a supporting electrolyte, but at a concentration too low to be observed. The ESR study of these solutions has shown that only the species $S_xO_{2x}^{-\cdot}$ with $x \leqslant 2$ and $S_yO_{2y}^{2-}$ with $y \leqslant 4$ could be present, which allows for the existence of $S_3O_6^{2-}$.

Another argument supporting the attribution of this band to $S_3O_6^{2-}$ is obtained from spectroelectrochemistry experiments. This also allows us to determine the mechanism of the formation of $S_3O_6^{2-}$, as it can be formed *via* two different reactions [reactions (4) or (5)].

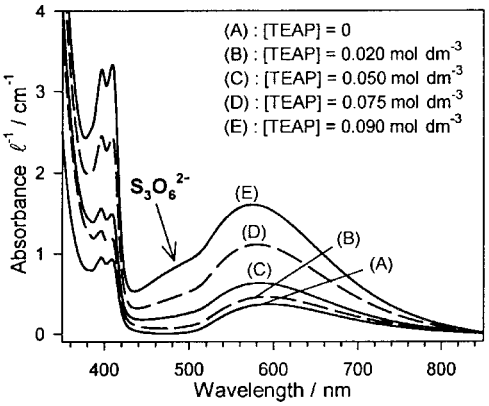

Fig. 7 UV/visible spectra of $Li(SO_2)_{1.5}$–TEAP–HMPA solutions with $[Li^+] = 0.005$ mol dm^{-3}, for different values of [TEAP]. In the presence of TEAP, a new absorption band is observed at about 500 nm; the absorbance of this band increases with [TEAP].

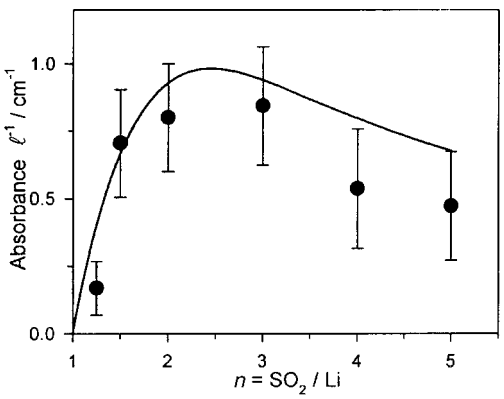

Fig. 8 Absorbance of the 498 nm band *vs.* n for $Li(SO_2)_n$–TEAP–HMPA solutions with $[Li^+] = 0.005$ mol dm^{-3} and [TEAP] = 0.1 mol dm^{-3}. (●) Experimental points, obtained from the decomposition of the spectra. For each value of n, at least three solutions were investigated, but only the mean value is plotted. The error bars take into account both the standard deviation of these measurements and the error due to the decomposition calculation. (——) Calculated line taking ε(498 nm) = 9500 cm^{-1} mol^{-1} dm^3, $K_f(S_3O_6^{2-}) = 625$ mol^{-1} dm^3, and shifting other equilibrium constant values by 50%.

The absorption band of $S_3O_6^{2-}$ at 498 nm is observed only in semi-infinite diffusion conditions, but not in thin layer conditions. This means that the species involved is formed in a reaction between a species generated at the electrode, and a species diffusing from the bulk of the solution towards the electrode: in thin layer conditions, there is no diffusion from the bulk, and the red complex is not observed. Moreover, the 498 nm band is observed only for polythionite solutions, not for SO_2 solutions. Therefore, the species diffusing from the solution is not SO_2 nor S_2O_4, but a reduced species.

Fig. 9(*b*) shows the variation of the absorbance at 498 nm, extracted from the 700 spectra recorded during the experiment. A second absorption band, at 370 nm, follows exactly the same variations [Fig. 9(*c*)]. This band was not observed during the spectrophotometric study of polythionite solutions at equilibrium, because it is located near the UV region, where

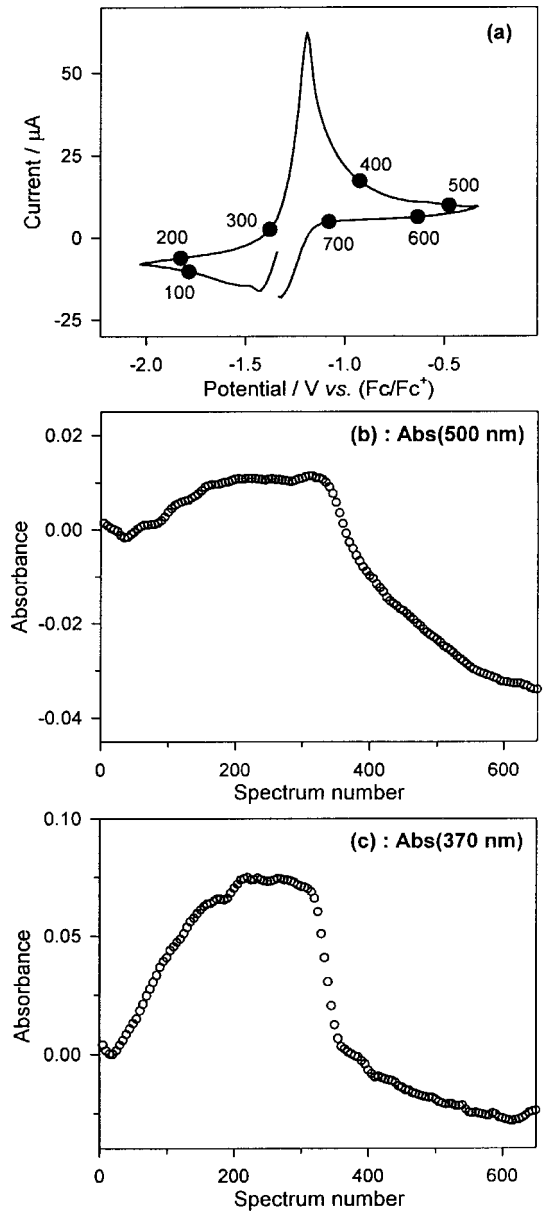

Fig. 9 Spectroelectrochemistry experiment on a $Li(SO_2)_n$–TEAP–HMPA solution with $[Li^+] = 0.005$ mol dm^{-3} and [TEAP] = 0.1 mol dm^{-3} in semi-infinite diffusion conditions. Initial cathodic scan, scan rate 5 mV s^{-1}, $T = 20$ °C, electrode: Pt disk, ∅ 5 mm. (*a*) Experimental voltammogram. The successively recorded spectra are numbered as indicated on the plot. (*b*) Variation of the absorbance at 500 nm during the experiment, *vs.* the spectrum number, that is, *vs.* time. (c) Variation of the absorbance at 370 nm during the experiment, as in (*b*).

the spectra could not be decomposed due to the too large number of bands. The absorbance of these two bands increases during the first part of the experiment, that is the reduction, and then decreases during the oxidation. Thus, the red complex is a reduced species, which is produced continuously during the cathodic scan of the voltammogram.

All these observations are coherent with the attribution of the 498 and 370 nm bands to $S_3O_6^{2-}$, and show that, in the course of an electrochemistry experiment, it is formed mainly by reaction between $SO_2^{-\cdot}$, generated at the electrode during the cathodic scan, and $S_2O_4^{-\cdot}$, diffusing from the bulk [reaction (4)].

Obtaining an estimation of the equilibrium constant of reaction (4) is more difficult than for the other reactions: in those cases, the area of the ESR signal of $S_2O_4^{-\cdot}$ allowed its concentration to be determined, and using these values, an estimation of the equilibrium constant of reactions (3) and (10) has been obtained. This method cannot be used here, because $S_3O_6^{2-}$ is not a radical species.

To deduce the concentration of $S_3O_6^{2-}$ from the absorbance of the 498 nm band, it is necessary to know the absorption coefficient of this band. If we suppose that it is not too different from that of $S_4O_8^{2-}$ at 595 nm (9500 cm^{-1} mol^{-1} dm^3), we obtain an estimation of $[S_3O_6^{2-}]$ *vs.* *n* for $[Li^+] = 0.005$ mol dm^{-3} and [TEAP] = 0.1 mol dm^{-3} (Fig. 8). Then, this curve is simulated using a model composed of reactions (2), (3), (8), (10) and (4). For the first four (the dimerization of SO_2, $SO_2^{-\cdot}$ and $S_2O_4^{-\cdot}$, and the formation of $S_2O_4^{-\cdot}$), the equilibrium constants in the absence of a supporting electrolyte have been determined. Assuming a value for $K_f(S_3O_6^{2-})$, the equilibrium constant of reaction (4), $[S_3O_6^{2-}]$ can be calculated. If the values of the other equilibrium constants are left unchanged, the calculated curve does not fit well to the experimental points, whatever the value used for $K_f(S_3O_6^{2-})$.

However, the increase of the ionic strength modifies the apparent value of the equilibrium constants.[40] Equilibria involving neutral species are shifted towards the dissociation of species, while for charged species, complexation is favored. The values of the equilibrium constants of the reactions composing the model have been determined in the absence of supporting electrolyte. In order to check if the present model is able to reproduce the variations of $[S_3O_6^{2-}]$ *vs.* *n*, the values of the equilibrium constants have been arbitrarily modified, to take approximately into account the influence of the increase of the ionic strength. For reaction (8), which involves only neutral species, the equilibrium constant has been decreased by 50%. All the other reactions of the model [reactions (2), (3), (10)] involve charged species and their respective equilibrium constants have been increased by 50%. If a value of $K_f(S_3O_6^{2-}) = 625$ mol^{-1} dm^3 is used for the equilibrium constant of reaction (4), the calculated curve of $[S_3O_6^{2-}]$ *vs.* *n* fits reasonably well to the experimental points (Fig. 8).

Obviously, this procedure only shows that it is possible to find a set of equilibrium constants for which the variation of $[S_3O_6^{2-}]$ is correctly described. Consequently, this confirms the existence of $S_3O_6^{2-}$, and the attribution of the 498 nm band to this species.

Conclusions

The ESR and spectrophotometric study of polythionite solutions $Li(SO_2)_n$–HMPA has led to the unambiguous identification of the blue and red complexes. We have shown that the blue complex is not $S_2O_4^{-\cdot}$, but its dimer species, $S_4O_8^{2-}$, contrary to the conclusions of all previous studies. On the other hand, the red complex was shown to be $S_3O_6^{2-}$, in agreement with the earlier interpretations. In HMPA, it is only observed in the presence of a supporting electrolyte, because of the increase of the ionic strength. The formation mechanism of $S_3O_6^{2-}$ by reaction between $SO_2^{-\cdot}$ and

$S_2O_4^{-\cdot}$ was shown to be kinetically favored at room temperature, relatively to the other possible mechanism of formation of $S_3O_6^{2-}$ [reaction (5)].

It can be noted that the colored species are $S_3O_6^{2-}$ and $S_4O_8^{2-}$, which are not radical species. The absorption bands of the radical species could not be identified clearly: $SO_2^{-\cdot}$ was shown to absorb in the UV region, and $S_2O_4^{-\cdot}$ probably does too. This study also shows that radical species are always present at low concentrations relative to their dimers. This explains why, in all the previous studies, the oxidation current is always low,[8,9,13–15] and this is one of the reasons why the electrochemical reduction of SO_2 is difficult to understand.

In conclusion, the spectroscopic study of polythionite solutions allowed us to identify the reduced species and the chemical reactions between these species. This is an important point towards the understanding of sulfur dioxide reduction, as these are the same reactions that are coupled to the electron transfers. Moreover, the quantitative study led to an estimation of the equilibrium constant of these reactions, which will be very helpful for the quantitative analysis of the electrochemistry experiments.

Acknowledgements

The authors are grateful to Dr F.-X. Sauvage for a critical reading of the manuscript. One of the authors (EP) wishes to thank the "Ministère de l'Education Nationale et de l'Enseignement Supérieur et de la Recherche" for granting her a doctoral scholarship.

References

1 E. M. Shembel and O. S. Ksenzhek, *Electrokhimiya*, 1986, **22**, 1680.
2 Y. Ein-Eli, S. R. Thomas and V. R. Koch, *J. Electrochem. Soc.*, 1997, **144**, 1159.
3 H. J. Wille, B. Kastening and D. Knittel, *J. Electroanal. Chem.*, 1986, **241**, 221.
4 F. Eugène, B. Langlois and E. Laurent, *New J. Chem.*, 1993, **17**, 815.
5 K. P. Dinse and K. Möbius, *Z. Naturforsch., Teil A*, 1968, **23**, 695.
6 R. G. Rinker and S. Lynn, *Ind. Eng. Chem.*, 1969, **8**, 338.
7 R. Bonnaterre and G. Cauquis, *J. Electroanal. Chem.*, 1971, **32**, 215.
8 R. P. Martin and D. T. Sawyer, *Inorg. Chem.*, 1972, **11**, 2644.
9 F. Magno, G. A. Mazzocchin and G. Bontempelli, *J. Electroanal. Chem.*, 1974, **57**, 89.
10 P. Bruno, M. Caselli and A. Traini, *J. Electroanal. Chem.*, 1980, **113**, 99.
11 V. D. Parker, *Acta Chem. Scand., Ser. A*, 1984, **37**, 423.
12 D. Knittel, *J. Electroanal. Chem.*, 1985, **195**, 345.
13 C. L. Gardner, D. T. Fouchard and W. R. Fawcett, *J. Electrochem. Soc.*, 1981, **128**, 2337.
14 C. L. Gardner, D. T. Fouchard and W. R. Fawcett, *J. Electrochem. Soc.*, 1981, **128**, 2345.
15 B. S. Kim and S. M. Park, *J. Electrochem. Soc.*, 1995, **142**, 26.
16 R. G. Rinker and S. Lynn, *J. Phys. Chem.*, 1968, **72**, 4706.
17 F. C. Laman, C. L. Gardner and D. T. Fouchard, *J. Phys. Chem.*, 1982, **86**, 3130.
18 A. Anantaraman, P. Archambault, R. Day and C. Gardner, *Proc. Electrochem. Soc.*, 1984, **84**, 231.
19 W. A. Adams, C. L. Gardner and D. T. Fouchard, in *Proceedings of the 7th International Raman Conference*, Ottawa, 1980, p. 202.
20 W. D. Harrison, J. B. Gill and D. C. Goodall, *J. Chem. Soc., Dalton Trans.*, 1979, 847.
21 E. Potteau, J.-P. Lelieur and E. Levillain, *New J. Chem.*, 1997, **21**, 521.
22 C. K. Mann, in *Electroanalytical Chemistry*, ed. A. J. Bard, Dekker, New York, 1969, vol. 3, p. 92.
23 D. F. Burow, in *The Chemistry of Non-aqueous Solvents*, ed. J. J. Lagowski, Academic Press, New York, 1966, vol. 3, p. 137.
24 C. G. Jung, F. Peeters, J. Castillo, S. Boué and A. Fontana, *J. Chem. Soc., Faraday Trans.*, 1995, **91**, 3809.
25 E. Potteau, E. Levillain and J.-P. Lelieur, *New J. Chem.*, 1999, **23**, 123.
26 F. Gaillard and E. Levillain, *J. Electroanal. Chem.*, 1995, **398**, 77.
27 G. Gritzner and J. Kuta, *Pure Appl. Chem.*, 1984, **56**, 869.
28 E. Levillain, P. Leghié, N. Gobeltz and J.-P. Lelieur, *New. J. Chem.*, 1997, **21**, 335.
29 W. H. Press, B. P. Flamery, S. A. Teukowski and W. T. Vetterling, *Numerical Recipes*, Cambridge University Press, Cambridge, 1984.
30 S. M. Lough and J. W. McDonald, *Inorg. Chem.*, 1987, **26**, 2024.
31 V. Pinon, E. Levillain and J.-P. Lelieur, *J. Magn. Reson.*, 1992, **96**, 31.
32 W. C. Hödgeman, J. B. Weinrach and D. W. Bennett, *Inorg. Chem.*, 1991, **30**, 1611.
33 R. Steudel and T. Steiger, *THEOCHEM*, 1993, **284**, 55.
34 H. S. Kim and M. T. Bowers, *J. Chem. Phys.*, 1986, **85**, 2718.
35 N. Berthe-Gaujac, I. Demachy, Y. Jean and F. Volatron, *Chem. Phys. Lett.*, 1994, **221**, 145.
36 N. Berthe-Gaujac, Y. Jean and F. Volatron, *Chem. Phys. Lett.*, 1995, **243**, 165.
37 D. L. Massart, B. G. M. Vandeginste, L. M. C. Buydens, S. De Jong, P. J. Lewi and J. Smeyers-Verbeke, *Handbook of Chemometrics and Qualimetrics, Part A*, Elsevier, Amsterdam, 1997, p. 180.
38 B. E. Barker and M. F. Fox, *Chem. Soc. Rev.*, 1980, **9**, 143.
39 Y. Geronov, R. V. Moshtev and B. Puresheva, *J. Electroanal. Chem.*, 1980, **108**, 335.
40 H. S. Harned and B. B. Owen, *The Physical Chemistry of Electrolytic Solutions*, Reinhold, New York, 1949, ch. 3 and 12.

Paper 9/03584B